




## Design, synthesis and docking study of 3,4-dihydropyrimidine-2-one derivatives as inhibitors of the Mitotic Kinesin, Eg5

Hossein Sadeghpour<sup>1\*</sup>; PhD , Ramin Miri<sup>2</sup>; PhD, Seyed Ahmad Ebadi<sup>3</sup>; PhD , Shima Mohammadebrahimi<sup>4</sup>; MSc, Elham Riazimontazer<sup>1,5\*</sup>; PhD 

<sup>1</sup>Department of Medicinal Chemistry, School of Pharmacy, Shiraz University of Medical Sciences, Shiraz, Iran.

<sup>2</sup>Medicinal and Natural Products Chemistry Research Center, Shiraz University of Medical Sciences, Shiraz, Iran.

<sup>3</sup>Department of Medicinal Chemistry, School of Pharmacy, Medicinal Plants and Natural Products Research Center, Hamadan University of Medical Sciences, Hamadan, Iran.

<sup>4</sup>Student Research Committee, Shiraz University of Medical Sciences, Shiraz, Iran.

<sup>5</sup>Biotechnology Research Center, Shiraz University of Medical Sciences, Shiraz, Iran.

### Abstract

A series of 3,4-dihydropyrimidine-2-one derivatives were designed and synthesized as monastrol analogs by Biginelli cyclocondensation of a  $\beta$ -keto compounds and aromatic aldehyde with urea or thio-urea. Biginelli cyclocondensation usually produces racemic mixtures of 3,4-dihydropyrimidine-2-ones. Enantiomers of 3,4-dihydropyrimidine-2-ones (R and S) often show different biological activities and may even have an opposite action profile. Therefore, developing of the stereoselective synthesis of 3,4-dihydropyrimidine-2-ones is one of the priorities of medicinal chemistry. Following observed diverse pharmacological effects of monastrol, 3,4-dihydropyrimidine-2-ones as new anti-cancer agents are the pharmacological category which improve and decrease the side effects of dihydropyrimidines especially resistance to chemotherapeutic drugs. 3,4-Dihydropyrimidine-2-ones followed their anticancer effects by inhibiting the kinesin motor protein. Because of the specific function of these proteins in mitosis, targeting the Kinesin spindle protein (KSP, or Eg5) as the most dramatic target of the mitotic kinesin family open up an opportunity for the progress of more selective antimetotics with an improved side effect profile. These facts prompted us to investigate if the effects of inhibitory enantiomers (R and S) of 3,4-dihydropyrimidine-2-ones could possibly differ from each other. Therefore, molecular docking of both R and S stereoisomers of 3,4-dihydropyrimidine-2-ones and monastrol was performed to study the interaction between inhibitors and the kinesin spindle protein binding site. According to docking studies, S stereoisomer of D<sub>2</sub> (SD<sub>2</sub>) has the best score among the synthesized compounds and shows probably more stable binding with the active site of the enzyme and can be considered as a candidate for biological evaluation.

**Keywords:** 3,4-Dihydropyrimidine-2-one, Biginelli reaction, Kinesin motor protein, Docking

Please cite this article as: Sadeghpour H, Miri R, Ebadi A, Mohammadebrahimi S, Riazimontazer E. Design, synthesis and docking study of 3,4-dihydropyrimidine-2-one derivatives as inhibitors of the Mitotic Kinesin, Eg5. Trends in Pharmaceutical Sciences. 2023;9(3):191-202. doi: 10.30476/TIPS.2023.98698.1195

### 1. Introduction

Cancer is a disorder resulting fundamental abnormalities in the regulations that control cell survival, proliferation and differentiation. Chemotherapy is a frequent treatment of many kinds of

cancer; however, by itself, it is able to improve the chances of survival only about 10-15% of all cancer patients.

In addition, development of drug resistance remains the major obstacles in the successful chemotherapy. Kinesins are a diverse two-headed superfamily of motor proteins found in eukaryotic cells that use the energy from hydrolysis of ATP to

*Corresponding Author:* Hossein Sadeghpour, Department of Medicinal Chemistry, School of Pharmacy, Shiraz University of Medical Sciences, Shiraz, Iran

Email: sadeghpurh@sums.ac.ir

generate force and movement along microtubules (MTs). Microtubules are dynamic linear polymers composed of  $\alpha$  and  $\beta$  tubulin dimmers. They are a cytoskeleton component with an important role in a number of cellular process including the movement of secretory vesicles, organelles, and intracellular macromolecular assemblies of kinesins in chromosome separation (mitosis and meiosis), and are the major constituents of mitotic spindles, which are used to pull apart eukaryotic chromosomes (1-7).

A sub-group of kinesins are the kinesin spindle enzyme (KSP) or Homo sapiens Eg5 (HsEg5) that are needed for proper spindle length and sliding microtubules apart through bipolar spindle formation during mitosis phase of cell division (8-10).

Mitotic spindle causes segregation of replicated DNA into two newly formed cells during mitotic phase (11). Any disorders in formation of spindle afford abnormal chromosomal segregation resulting in mitotic arrest (12).

In addition, Eg5 is expressed more in transformed cells than in primary cells and its overexpression is higher in numerous proliferative tissues, such as leukemia, solid tumors including breast, colon, lung, ovary, uterus, bladder and pancreatic cancers, as compared to nonproliferative tissues. Almost, no Eg5 is present in nonproliferative tissues (13-18). Therefore, it could be concluded that Eg5 has been viewed as a potential target for cancer treatment (19).

The first effect of Eg5 inhibition is accumulation of monopolar spindles known as “monasters” surrounded by condensed chromosomes, leading to prevent centrosomal separation and so mitotic block without disturbing the microtubules. This form of mitotic arrest in a monopolar stage leads to absolute cell death (apoptosis) of many cancer cells without affecting non-proliferating and normal cells (20, 21). Comparing to current antimicrotubule agents such as taxanes, vinca alkaloids, and epothilones, it can be predicted that inhibitors of Eg5 may not have serious unwanted side effects (22). Traditional antimiotic agents interfere with microtubules and affect both normal and proliferating cells. The disruption of microtubule formation can have toxic side effects, includ-

ing hair loss, body weight loss, and neurotoxicity (23-25). There is no risk of neuropathic side effects associated with Eg5 inhibitors because it is not expressed in the adult peripheral nervous system, unlike other tubulin target agents (26, 27).

Eg5 inhibitors are effective against mechanisms by which cancer cells develop resistance to chemotherapeutic drugs such as taxols. They may result from tubulin mutations or P-glycoprotein (Pgp)-mediated cellular efflux. The gene for P-glycoprotein, called MDR-1 is an energy-dependent pump that is capable of actively expelling chemotherapeutic agents from within cells. Overexpression of MDR-1 causes multidrug resistant phenotype exhibited by cells (28).

A variety of Eg5 inhibitors have been studied in two groups, as allosteric binding inhibitors (ATP uncompetitive) and ATP competitive with the majority of the first one (29, 30). The first group of compounds, adociasulfate-2, that inhibited kinesin was extracted from a marine sponge, Haliclona (also known as adosia) species (31). This sponge secretes a poison due to protect itself against aggressive effects. The poison is adociasulfate-2 that inhibits basal and MT-stimulated ATPase activity of Eg5, and is reported as inhibitor of some kinesins which exhibited nonspecific inhibitory activity.

Recently, several varieties of of Eg5 inhibitors have been reported (32-37). Mayer et al. had previously identified a dihydropyrimidine (DHPM) structure, (S)-monastrol, the first specific KSP inhibitor and the first known cell-permeable small molecule that has been shown to be an ATP uncompetitive allosteric inhibitor (38). Due to the potent antitumor activity of DHPM by Eg5 inhibition we decided to synthesize several structural analogues, in part to generate inhibitors with improved potency.

In this project, some new racemic 3,4-dihydropyrimidine-2-one derivatives were designed and synthesized by Biginelli cyclocondensation of a  $\beta$ -keto compound and aromatic aldehyde with urea. Because of different biological activity and side effects of dihydropyrimidine stereoisomers especially resistance to chemotherapeutic medicines, enantiomers of 3,4-dihydropyrimidine-2-ones (R and S) were evaluated by docking studies. Docking analysis was performed to clarify the binding

affinity of compounds against the active site and helped in revealing the potential mode of action through their interactions. Both configuration R and S in the binding site of Eg5 were investigated from the docking method to find out which enantiomer has the most prominent inhibitory activity. This method could potentially uncover the ways in which the studied stereoisomer inhibitors and Eg5 interact, which could lead to the development of Eg5 inhibitors that could be used to treat cancer. The mode of interaction between receptor and ligand and predicted free energy can be effectively used for design of bioactive compounds.

## 2. Experimental protocols

All solvents and reagents were purchased from Sigma or Merck Chemical Companies. Reactions were monitored by thin-layer chromatography (TLC) using coated silica gel plates (Merck, Germany), and the spots were detected under UV light (254 nm). The melting point was measured on an Electro Thermal 9200 micro melting point apparatus and reported uncorrected. IR spectra (KBr-disc) were recorded using a Perkin Elmer Spectrometer (Germany).  $^1\text{H}$  and  $^{13}\text{C}$  NMR spectra were acquired in DMSO on a Bruker Avance DPX 500 instrument (Germany). Chemical shifts are expressed in  $\delta$  (ppm) relative to TMS as internal standard. Coupling constants are given in Hz. The splitting patterns are designed as s; singlet, d; doublet, t; triplet, m; multiplet. Mass spectra were recorded on a Hewlett Packard (HP) Mass Spectrometer.

### 2.1. General procedure for Synthesis of 3,4-dihydropyrimidine-2-ones

General procedure is consist of combination of 2 mmol of  $\beta$ -keto compound ( $\text{C}_{1-8}$ ) and 2 mmol of aromatic aldehyde ( $\text{A}_{1-8}$ ) with 3 mmol of urea or thiourea (B) in 20 ml of solvent (ethanol or acetonitril) in the presence of an appropriate Lewis acid such as  $\text{FeCl}_3$  (0.07 g) as a catalyst. The reaction was refluxed during 24 h. After the accomplishment of reaction, solvent was evaporated under vacuum and the pure product obtained by silica gel chromatography with petroleum ether and ethylacetate (75:25) and then crystallized at diethylether to afford  $\text{D}_{1-8}$  as a pure powder in 19

to 45 % yield. Finally the structures confirmed by spectroscopic methods such as IR,  $^1\text{H}$ -NMR and Mass spectroscopy. The overall scheme of the reaction brought in Scheme 1. Yield of all products come in Table 1.

### 2.2. 5-benzoyl-6-methyl-4-(thiophene-2-yl)-1,2,3,4-tetrahydropyrimidine-2-one ( $\text{D}_1$ )

Compound  $\text{C}_1$  was treated with  $\text{A}_1$  and B according to the general cyclization procedure to give the desired product  $\text{D}_1$  as a yellow powder in 19.44% yield;  $^1\text{H}$ -NMR (400 MHz, DMSO):  $\delta$  (ppm) 1.67 (s, 3H,  $\text{CH}_3$ -DHPM), 5.56 (d, 1H,  $\text{C}_4\text{H}$ -DHPM,  $J=3.2$  Hz), 6.86 (dd, 1H,  $\text{C}_3'\text{H}$ -thiophen,  $J=3.2, 1.2$  Hz), 6.93 (dd, 1H,  $\text{C}_4'\text{H}$ -thiophen,  $J=5.2, 3.2$  Hz), 7.38 (dd, 1H,  $\text{C}_5'\text{H}$ -thiophe,  $J=5.2, 1.2$  Hz), 7.44-7.55 (comp., 5H, H-phenyl), 7.80 (s, 1H,  $\text{N}_3\text{H}$ ), 9.33 (s, 1H,  $\text{N}_1\text{H}$ ); MS  $m/z$  (%): 298 [ $\text{M}^+$ ] (65.5), 283 (13.7), 193 (41.3), 105 (71.2), 77 (100); IR(KBr)  $\nu$  ( $\text{cm}^{-1}$ ): 3288.81 (N-H, DHPM), 2925.24 (C-H, aromatic), 2854.14 (C-H, aliphatic), 1698.17 (C=O, keton), 1676.12 (C=O, amide).

### 2.3. 5-benzoyl-6-methyl-4-(naphthalene-2-yl)-1,2,3,4-tetrahydropyrimidine-2-one ( $\text{D}_2$ )

Compound  $\text{C}_2$  was treated with  $\text{A}_1$  and B according to the general cyclization procedure to give the desired product  $\text{D}_2$  as a yellow crystal in 25.16% yield;  $^1\text{H}$ -NMR (400MHz, DMSO):  $\delta$  (ppm) 1.71 (s, 3H,  $\text{CH}_3$ -DHPM), 5.52 (d, 1H,  $\text{C}_4\text{H}$ -DHPM,  $J=3.2$  Hz), 7.40-7.52 (comp., 8H, CH-naphthalen and CH-phenyl), 7.63 (s, 1H, CH-naphthalen), 7.85-7.91 (comp., 4H, CH-naphthalen and  $\text{N}_3\text{H}$ ), 9.24 (bs, 1H,  $\text{N}_1\text{H}$ ); MS ( $m/z$ , %): 342 [ $\text{M}^+$ ] (76.1), 237 (47.7), 215 (45.45), 105 (95.45), 77 (100); IR(KBr)  $\nu$  ( $\text{cm}^{-1}$ ): 3239.29 (N-H, DHPM), 3112.96 (C-H, aromatic), 1699.12 (C=O, keton), 1630.11 (C=O, amide).

### 2.4. 5-benzoyloxycarbonyl-6-methyl-4-(naphthalene-2-yl)-1,2,3,4-tetrahydropyrimidine-2-one ( $\text{D}_3$ )

Compound  $\text{C}_3$  was treated with  $\text{A}_3$  and B according to the general cyclization procedure to give the desired product  $\text{D}_3$  as a white powder in 42.21% yield;  $^1\text{H}$ -NMR (400MHz, DMSO):  $\delta$  (ppm) 2.32 (s, 3H,  $\text{CH}_3$ -DHPM), 4.99(d, 1H,

CH<sub>2</sub>phenyl, J=12.8 Hz), 5.06 (d, 1H, CH<sub>2</sub>phenyl, J=12.8 Hz), 5.36 (d, 1H, C<sub>4</sub>H-DHPM, J=2.8 Hz), 7.11-7.24 (comp., 5H, CH-phenyl), 7.42-7.52 (comp., 3H, CH-naphthalen), 7.62 (s, 1H, CH-naphthalen), 7.80-7.89 (comp., 4H, CH-naphthalen and N<sub>3</sub>H), 9.32 (s, 1H, N1H); MS (m/z, %) : 372 [M<sup>+</sup>] , (5.8), 281 (45.88), 245 (15.2), 128 (11.7), 91 (100) ; IR(KBr)  $\nu$  (cm<sup>-1</sup>) : 3223.68 (N-H, DHPM), 3113.33 (C-H, aromatic), 2979.95 (C-H, aliphatic), 1709.77 (C=O, keton), 1686.83 (C=O, amide).

#### 2.4. 5-allyloxy carbonyl-6-methyl-4-(naphthalene-2-yl)-1,2,3,4-tetrahydropyrimidine-2-one (D<sub>4</sub>)

Compound C<sub>4</sub> was treated with A<sub>4</sub> and B according to the general cyclization procedure to give the desired product D<sub>4</sub> as a white powder in 13.39% yield; 1H-NMR (400MHZ, DMSO):  $\delta$  (ppm) 2.33 (s, 3H, CH<sub>3</sub>-DHPM), 4.49 (d, 2H, COOCH<sub>2</sub>, J=5.2 Hz), 5.07 (dd, 1H, CHgeminal-CH=CH<sub>2</sub>, J=10.4, 1.6 Hz), 5.11 (dd, 1H, CHgeminal-CH=CH<sub>2</sub>, J=17.2, 1.6 Hz), 5.37 (d, 1H, C<sub>4</sub>H-DHPM, J=3.2 Hz), 5.78-5.88(ddt, 1H, CH=CH<sub>2</sub>, J=17.2, 10.4, 5.2 Hz), 7.45-7.52 (comp., 3H, CH-naphthalen), 7.69 (s, 1H, CH-naphthalen), 7.87-7.91 (comp., 4H, CH-naphthalen and N<sub>3</sub>H), 9.32 (d, 1H, N1H, J=1.2 Hz); MS (m/z, %) : 322 [M<sup>+</sup>] , (24.2), 281 (100), 237 (48), 195 (97.5), 127 (40.2), 41 (15.85) ; IR(KBr)  $\nu$  (cm<sup>-1</sup>) : 3232.56 (N-H, DHPM), 3101.29 (C-H, aromatic), 2942.63 (C-H, aliphatic), 1704.33 (C=O, keton), 1650.77 (C=O, amide).

#### 2.5. 5-benzoyl-4-(4-methoxyphenyl)-6-methyl-3,4-dihydropyrimidin-2(1H)-one (D<sub>5</sub>)

Compound C<sub>5</sub> was treated with A<sub>5</sub> and B according to the general cyclization procedure to give the desired product D<sub>5</sub> as a yellow crystal in 41.20% yield; 1H-NMR (400MHZ, DMSO):  $\delta$  (ppm) 1.68 (s, 3H, CH<sub>3</sub>-DHPM), 3.71 (s, 3H, CH<sub>3</sub>O), 5.25 (d, 1H, C<sub>4</sub>H-DHPM, J=3.2 Hz), 6.86 (d, 2H, C<sub>3</sub>'H, C<sub>5</sub>'H-aromatic, J=8.4 Hz), 7.12 (d, 2H, C<sub>2</sub>'H, C<sub>6</sub>'H-aromatic, J=8.4 Hz), 7.41-7.54 (comp., 5H, CH-phenyl), 7.75 (bs, 1H, N<sub>3</sub>H), 9.15 (s, 1H, N1H) ; MS (m/z, %) : 322.2[M<sup>+</sup>] , (100), 307.2 (35.8), 217 (50.3), 105 (36.6), 77 (39.1) ; IR(KBr)  $\nu$  (cm<sup>-1</sup>) : 3282.48 (N-H, DHPM), 2996.16 (C-H, aromatic), 2927.67 (C-H, aliphatic), 1708.8

(C=O, keton), 1674.28 (C=O, amide)

#### 2.6. 5-ethyloxy carbonyl-6-methyl-4-(naphthalene-2-yl)-1,2,3,4-tetrahydropyrimidine-2-one (D<sub>6</sub>)

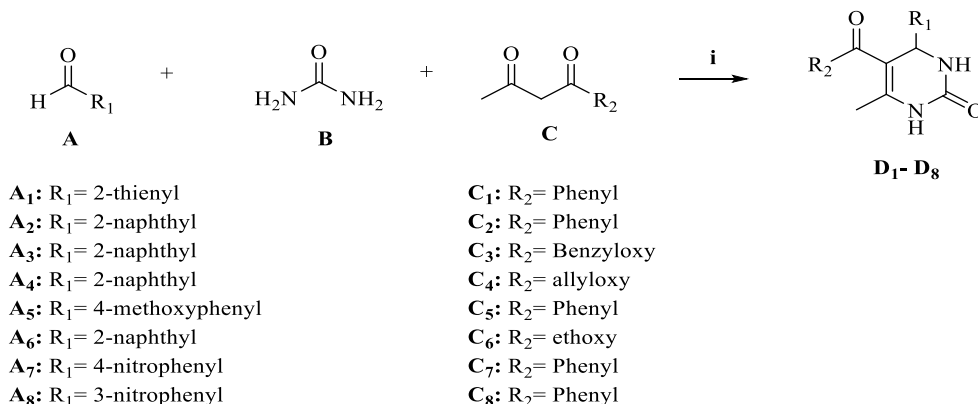
Compound C<sub>6</sub> was treated with A<sub>6</sub> and B according to the general cyclization procedure to give the desired product D<sub>6</sub> as a white powder in 14.35% yield; 1H-NMR (400MHZ, DMSO):  $\delta$  (ppm) 1.08 (t, 3H, -OCH<sub>2</sub>CH<sub>3</sub>, J=7.2 Hz), 2.30 (s, 3H, CH<sub>3</sub>-DHPM), 3.97 (q, 2H, -OCH<sub>2</sub>CH<sub>3</sub>, J=7.2 Hz), 5.33 (d, 1H, C<sub>4</sub>H-DHPM, J=3.2 Hz), 7.44-7.50 (comp., 3H, CH-naphthalen), 7.68 (s, 1H, CH-naphthalen), 7.86-7.91 (comp., 4H, CH-naphthalen and N<sub>3</sub>H), 9.28 (s, 1H, N1H) ; MS (m/z, %) : 310 [M<sup>+</sup>] (79.16), 281 (82.5), 264.1 (28.3), 237.2 (61.6), 183.3(100), 155.1 (38.3) ; IR(KBr)  $\nu$  (cm<sup>-1</sup>): 3222.83 (NH-DHPM), 3100.3 (C-H, aromatic), 2929.91 (C-H, aliphatic), 1704.54 (C=O, keton), 1651.55 (C=O, amide).

#### 2.7. 5-benzoyl-6-methyl-4-(4-nitrophenyl)-3,4-dihydropyrimidin-2(1H)-one (D<sub>7</sub>)

Compound C<sub>7</sub> was treated with A<sub>7</sub> and B according to the general cyclization procedure to give the desired product D<sub>7</sub> as a beige crystal in 25.2% yield; 1H-NMR (400MHZ, DMSO):  $\delta$  (ppm): 1.66 (s, 3H, CH<sub>3</sub>-DHPM), 5.43 (d, 1H, C<sub>4</sub>H-DHPM, J=3.2 Hz), 7.42-7.51 (comp., 5H, CH-phenyl), 7.52 (d, 2H, C<sub>2</sub>'H, C<sub>6</sub>'H-nitrophenyl, J=8.8 Hz), 8.00 (bs, 1H, N<sub>3</sub>H), 8.21 (d, 2H, C<sub>3</sub>'H, C<sub>5</sub>'H-nitrophenyl, J=8.8 Hz), 9.38 (s, 1H, N<sub>1</sub>H) ; MS (m/z, %) : 337.2 [M<sup>+</sup>] (7.07), 290 (35.35), 232 (15.15), 215 (54.54), 105 (82.82), 77(100); IR(KBr)  $\nu$  (cm-1): 3284.61 (N-H,DHPM), 3072.86 (C-H, aromatic), 2936.72 (C-H, aliphatic), 1710.53 (C=O, keton), 1677.09 (C=O, amide), 1533.15, 1346.35 (NO<sub>2</sub>).

#### 2.8. 5-benzoyl-6-methyl-4-(3-nitrophenyl)-3,4-dihydropyrimidin-2(1H)-one (D<sub>8</sub>)

Compound C<sub>8</sub> was treated with A<sub>8</sub> and B according to the general cyclization procedure to give the desired product D<sub>8</sub> as a beige crystal in 12.07% yield; 1H-NMR (400MHZ, DMSO):  $\delta$  (ppm): 1.68 (s, 3H, CH<sub>3</sub>-DHPM), 5.45 (d, 1H, C<sub>4</sub>H-DHPM, J=3.2 Hz), 7.42-7.54 (comp., 5H, CH-phenyl), 7.65 (dd, 1H, C<sub>5</sub>'H-nitrophenyl, J=8, 7.6 Hz), 7.72 (dd, 1H, C<sub>6</sub>'H-nitrophenyl, J=7.6,



**Scheme 1.** Reagents and conditions: (i) FeCl<sub>3</sub>, acetonitril, reflux.

2.4 Hz), 8.04 (bs, 1H, N3H), 8.09 (m, 1H, C<sub>2</sub>'H-nitrophenyl), 8.13 (ddd, 1H, C<sub>4</sub>'H-nitrophenyl, J=8, 2.4, 1.2 Hz), 9.41 (d, 1H, N1H, J=1.6 Hz); MS (m/z, %): 337 [M<sup>+</sup>] (48.9), 322 (21.27), 232 (26.59), 215 (52.1), 105 (81.9), 77 (100); IR(KBr)  $\nu$  (cm<sup>-1</sup>): 3300.91 (N-H, DHPM), 2925.94 (C-H, aliphatic), 1706.49 (C=O, keton), 1676.18 (C=O, amide), 1574.66, 1351.41 (NO<sub>2</sub>).

### 2.9. Docking simulation method

Since different 3D-structures were released for KSP, docking validation was used to pick a proper x-ray structure for docking simulation. From these complexes, 11 PDB codes for KSP were chosen from Protein Data Bank (<http://www.rcsb.org>). All the retrieved PDB codes were subjected to self-docking validation test. In this step, the cognate ligands were re-docked on their corresponding 3D structures and the best pose of docking was superimposed with the native conformation of the ligand at crystallographic state. Amongst all the retrieved PDB codes 1Q0B, 1X88, 2IEH, 2X7C, 2X7D, 2X7E and 3K5E were selected based on root-mean-square deviation (RMSD) values as shown in Table 2. PDB code 1X88 complexed with monastrol as a cognate ligand was selected in this investigation. The compound structures were drawn by chem office 3D program and were optimized by AM1 semiempirical calculation method. After that, charge calculation was done and the ligands were saved in pdbqt format. To prepare protein for docking simulation, at first, the amino acid chains were kept and the water molecules and co-crystallized ligand were removed. Afterward, the polar hydrogen was add-

ed to the receptor and the resulting protein was subjected to minimization. The prepared protein was saved in pdbqt format. The true 3D space (grid box) containing active site was considered for KSP enzyme.

All preparation was done using Auto Dock Tools package (1.5.6). Cross-docking simulations were performed using bash scripting in linux operating system. Autodock Vina (1.1.2) (<http://vina.scripps.edu/>) was used for docking within a box defined by following parameters. The grid box with the size of 30×30×30 was determined and the box was centered on co-crystallized ligand. The center of grid box was determined as [x=42.21, y=26.49, z=112.05] for 1X88. The exhaustiveness was set to 100 and the other docking parameters were set as default. At the end of cross-docking simulations, the best docking poses were selected for further analysis of enzyme-inhibitor interactions (42).

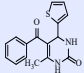
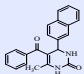
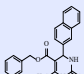
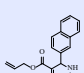
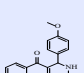
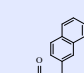
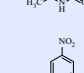
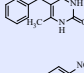
## 3. Results and discussion

### 3.1. Chemistry

The Biginelli cyclocondensation (39) of a  $\beta$ -keto compound (C<sub>1-8</sub>), aromatic aldehyde (A<sub>1-8</sub>) with urea or thiourea (B) (9) in the presence of FeCl<sub>3</sub> afforded target compounds D<sub>1-8</sub> (Scheme 1). The reaction was refluxed in appropriate solvent (ethanol or acetonitrile) for 24 h. Once the reaction was finished, the solvent was evaporated from the mixture in a vacuum. The crude product was purified by silica gel chromatography using n-hexane/ethylacetate to get the final products. The yield of reactions was 19-45% (Table 1).

The key step of this novel one pot, three-component synthesis involves the acid-catalyzed

**Table 1.** The results achieved from synthesis of 3,4-dihydropyrimidine-2-one derivatives

Comp.	R1	R2	Rf	Product	B.P.	Yield	color
D1	2-thienyl	Phenyl	0.22		203-204	19.44%	Yellow powder
D2	2-naphthyl	Phenyl	0.20		269-270	25.16%	Yellow crystal
D3	2-naphthyl	Benzyloxy	0.33		214-215	42.21%	White Powder
D4	2-naphthyl	Allyloxy	0.32		202-204	13.39%	White Powder
D5	4-methoxyphenyl	Phenyl	0.3		243-245	41.2%	Yellow Crystal
D6	2-naphthyl	Ethoxy	0.26		210-211	14.35%	White Powder
D7	4-nitro phenyl	Phenyl	0.18		249-252	25.2%	Beige crystal
D8	3-nitrophenyl	Phenyl	0.20		239-245	12.07%	Beige crystal

formation of an N-acyliminium ion intermediate from the aldehyde and urea precursors (40). In continue, iminium ion interact by  $\beta$ -keto compound through its enol tautomer and produces open-chain ureide. Ureide through an intramolecular cyclization turns into the hexahydropyrimidine. Acid-catalyzed removal of water from hexahydropyrimidine leads to the final product 3,4-dihydropyrimidine-2-one.  $\alpha$ -Amidoalkylation, or more specifically  $\alpha$ -ureidoalkylation are the mechanism

of these reactions (41).

### 3.2. Molecular docking study of 3,4-dihydropyrimidine-2-one stereoisomers with KSP enzyme active site

Docking is a method which predicts the most stable form of receptor-ligand by using genetic algorithm. The mode of interaction between receptor and ligand and predicted free energy can be effectively used for design of bioactive

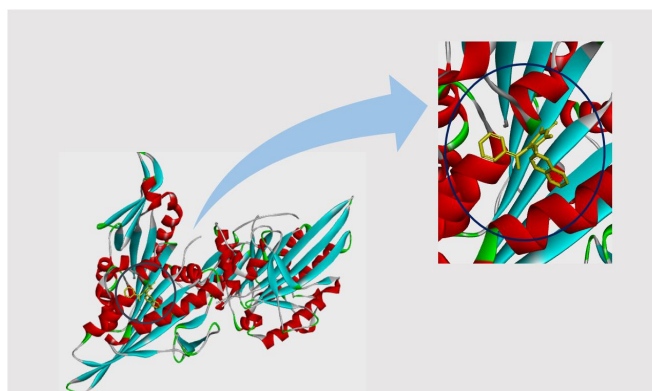


**Figure 1.** The full structure and magnification of KSP enzyme active site, PDB code: 1X88.

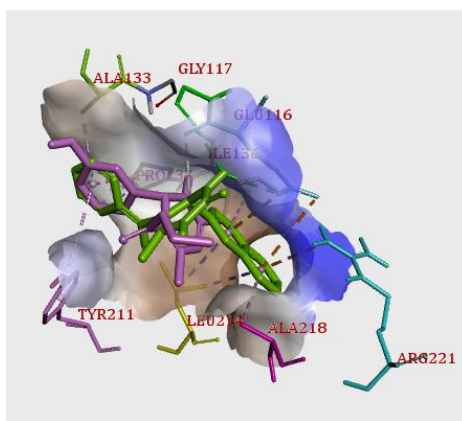
**Table 2.** RMSD values and predicted binding energies of synthesized 3,4-dihydropyrimidine-2-one stereoisomers derivatives in compare with monastrol as the standard compound.

PDB Code	RMS-Dof self-docking	Binding Energy (Kcal.mol <sup>-1</sup> )																	
		RD <sub>1</sub>	RD <sub>2</sub>	RD <sub>3</sub>	RD <sub>4</sub>	RD <sub>5</sub>	RD <sub>6</sub>	RD <sub>7</sub>	RD <sub>8</sub>	SD <sub>1</sub>	SD <sub>2</sub>	SD <sub>3</sub>	SD <sub>4</sub>	SD <sub>5</sub>	SD <sub>6</sub>	SD <sub>7</sub>	SD <sub>8</sub>	Mon	
1q0b	1.21	-9	-10	-10.5	-9.5	-9.4	-9.2	-9.5	-10	-8.9	-11.5	-8.1	-9.6	-9.8	-9.4	-10	-10.5	-7.9	
1x88	1.15	-9	-10.1	-10.2	-9.4	-9.5	-9.1	-9.6	-9.5	-9.1	-11.6	-10	-9.7	-9.9	-9.4	-10	-10.5	-8.1	
2ieh	0.17	-9.5	-10.6	-10.3	-9.3	-9.2	-9.1	-9.3	-9.1	-8.8	-11.4	-10.5	-9.7	-9.8	-9.5	-10	-10.6	-8	
2x7c	0.33	-8.8	-10	-10.4	-9.2	-9.5	-9	-9.6	-9.4	-9	-11.4	-10.2	-9.6	-9.8	-9.3	-10	-10.5	-7.8	
2x7d	0.66	-9.2	-11	-10.6	-9	-9.3	-8.7	-9.4	-9.2	-8.8	-11.6	-10.4	-9.7	-9.9	-9.6	-10.1	-10.5	-7.9	
2x7e	0.46	-8.9	-10.7	-10.3	-9.3	-8.8	-8.9	-9	-9.5	-8.3	-11.1	-9.8	-9.3	-9.4	-9	-9.3	-9.9	-7.3	
3k5e	0.33	-8.8	-9.9	-10.5	-9.1	-9.4	-8.3	-9.5	-9.3	-8.9	-11.6	-10.4	-9.6	-9.9	-9.5	-10.2	-10.5	-7.7	

compounds. The overall goal of this docking research project is the discovery of binding affinity of enantiomers of 3,4-dihydropyrimidine-2-one analogues to target enzyme. Binding capability of synthesized 3,4-dihydropyrimidine-2-one stereoisomers and monastrol as a control compound have investigated with KSP enzyme active site. Docking process of designed compounds with receptor is done by means of AutoDock Vina (1.1.2). Therefore, docking simulation of these compounds as anticancer agents with KSP as the target has been done to study potential possibility of binding of both stereoisomers R and S. For this purpose, seven 3D X-ray crystal structures of KSP were retrieved from Protein Data Bank (PDB) as a co-crystallized complex with monastrol and other similar structures. All of them were selected based on optimal self-docking criteria of RMSD < 2 Å described in Table 2. To determine the accuracy of docking process, the known co-crystallized inhibitor (monastrol) was excluded from the selected

crystalline 1X88 complex and re-docked into the active site.

The parameters obtained during the validation phase were used to cross-dock the synthesized compounds. Following completion of the cross-docking simulation, the best pose for the most prominent compound was selected for visualization and analysis. The findings of the cross-docking investigation concerning binding energies and RMSD values displays in Table 2 for each PDB codes. According to the predicted free energy by Autodock program, S and R stereoisomers have almost proximate binding affinity into the receptor active site, however, the binding energy of S isomers are less than R isomers. Due to this fact, it could be concluded that possibly S isomers of this group of compounds especially D<sub>2</sub> (SD<sub>2</sub>) have more important role in biological activity (Table 2). The results of this study demonstrate that the docked structures could be fit in an acceptable way with x-ray crystal structure. All interactions

**Figure 2.** Superimposition of the most favorable docked conformation SD<sub>2</sub> on dock pose of cocrystallized ligand, PDB code: 1X88, RMSD=1.15 Å.

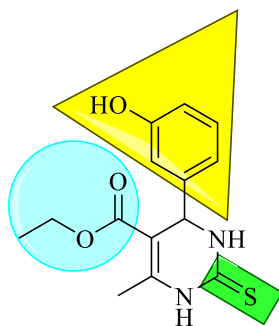


**Figure 3.** The structure of monastrol as the standard compound and as the basis for designing new analogues with modification sites.

that are used for prediction of binding energy are hydrophobic interactions and hydrogen bond between ligand and receptor. Based on these data, it is possible to design the same structures with more binding potency to enzyme's active site. The full structure of KSP receptor and magnification of the binding pocket of KSP receptor is shown in Figure 1. After docking process and evaluating each docked pose, superimposition of the most favorable docked conformation SD<sub>2</sub> on co-crystallized conformation, monastrol, is depicted in Figure 2. As shown in this figure, the docked structure was fitted in a good agreement way to active site of target enzyme with x-ray crystal structure which demonstrated the reliability of docking process with RMSD of 1.15 Å.

Monastrol was the first compound of 3,4-dihydropyrimidine-2-one derivatives, which was used as the basis for designing new analogues using bioisoster modification in this scaffold as a KSP enzyme inhibitor. In this study monastrol

investigated as a control compound (Figure 3). Monastrol make a hydrogen bond through hydrogen group with amino acid residues Glu116, and have alkyl and pi-alkyl bond through methyl group with Ala133, Pro137, Leu214 and Ala218 (Figure 4). To optimize its interactions with the receptor, KSP, critical hydrophobic interactions and hydrogen bonds were taken into consideration. The modifications were focused on improving these interactions. One of the initial modifications involved replacing the thiourea moiety in monastrol with urea. This was done because urea is known to be more biocompatible and tolerable than thio-urea. Additionally, urea has more favorable hydrogen bonding properties. Another modification was made to the aromatic site of the parent compound, monastrol. In this case, more lipophilic moieties were introduced in order to enhance the pi-pi interactions within the active site. Another modification involved replacing the ethyl ester group with other carbonyl substituents. The aim of these modifica-

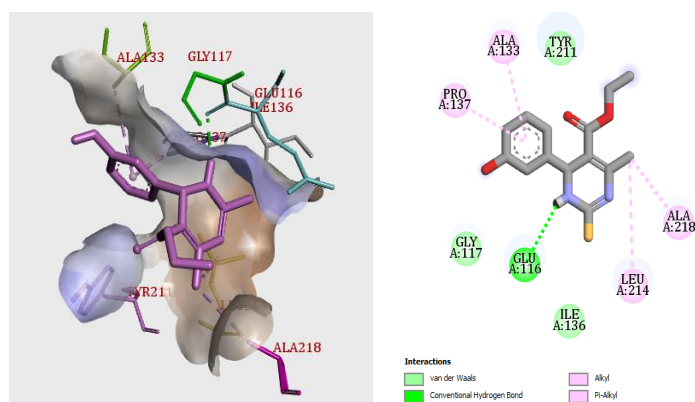


**Figure 4.** Schematic representation of monastrol interaction with KSP enzyme active site, PDB code: 1X88.



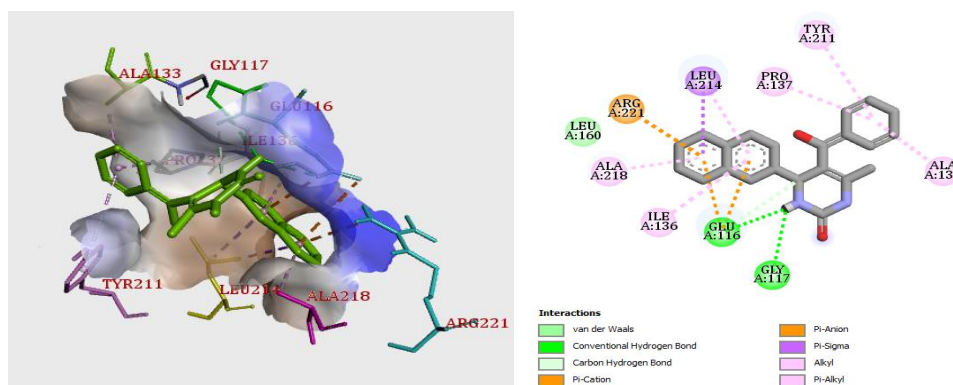


**Figure 5.** 3D (left) and 2D (right) schematic representation of interactions of stereoisomer SD<sub>2</sub> with KSP enzyme active site, PDB code: 1X88.

tions was to enhance the interactions between the ligand and the receptor. The overall goal of these modifications is to enhance hydrophobic interactions and hydrogen bonding between the modified compounds and the receptor, KSP. According to the obtained results of docking process, interaction energy of D<sub>2</sub> was lower than other compounds. Accordingly, interaction mode of this compound with enzyme active site is depicted in Figure 5. On the other way, S isomer of this compound make hydrophobic bond with active site through 2-naphthyl ring, phenyl ring and dihydropyrimidinone with amino acid residues Ile136, Ala133, Leu214, Glu116, Gly117, Pro137, and Tyr211. On the other hand, SD<sub>2</sub> makes a hydrogen bond through its dihydropyrimidinone ring with residues Glu116. This isomer establish  $\pi$ -cation bond through its 2-naphthyl ring and phenyl ring with residues Arg221 and Glu116, respectively (Figure 5, right). As it can be seen from the results of interaction for 1X88 PDB code, SD<sub>2</sub> showed that this ligand was well oriented towards the active site.

Based on the different substituents on dihydropyrimidinone structure, structure activity relationship of these compounds can be discussed. Amongst D<sub>1-8</sub>, it can be concluded that SD<sub>2</sub>, SD<sub>5</sub>, SD<sub>7</sub> and SD<sub>8</sub> are prominent predicted structure due to the lower binding energy. The results revealed that the inhibitory activity for Eg5 could be increased with the phenyl substituent at position 5 especially about D<sub>2</sub> with the naphthyl group at position 4. Binding of these compounds with ac-

tive site of receptor accomplish by hydrophobic interaction in which the effect has been perceived in studied substituents.

#### 4. Conclusion

In conclusion, a series of 3,4-Dihydropyrimidine-2-one stereoisomer derivatives as a new anti-cancer agents were designed and synthesized in this study. Because of different biological activity and side effects of dihydropyrimidine stereoisomers especially resistance to chemotherapeutic drugs, enantiomers of 3,4-dihydropyrimidine-2-ones (R and S) were investigated by docking studies. Molecular docking were carried out to find the optimal configuration of each inhibitor in the KSP binding site. The molecular modeling studies supported that stereoisomer SD<sub>2</sub> as the most prominent inhibitor could be selected to elucidate the interaction binding modes and further detailed analysis. Moreover, the results derived from molecular docking exhibited detailed information of residues in the binding pocket and confirmed that the hydrogen bond and hydrophobic interaction play a significant role in the binding of inhibitors to KSP. On the basis of mentioned interactions, it could be concluded that the interaction of these synthesized inhibitors with amino acid residues of enzyme active site is similar to monastrol as a control compound. Considering the similarity of interaction mode with residues it could be understand that these compounds possibly bind with enzyme active site.

## Acknowledgment

The study was financially supported by the office of vice-chancellor for research of Shiraz University of Medical Sciences. The authors would like to thank all the kind research staff of

Shiraz University of Medical Sciences who participated in the conduct of the present study.

## Conflict of Interest

The authors declare no conflict of interest.

---

## References

1. Wordeman L. The kinesin superfamily. Cytoskeleton and Human Disease: Springer; 2012. p. 55-72.
2. Hirokawa N. Kinesin and dynein superfamily proteins and the mechanism of organelle transport. *Science*. 1998 Jan 23;279(5350):519-26. doi: 10.1126/science.279.5350.519. PMID: 9438838.
3. Endow SA. Microtubule motors in spindle and chromosome motility. *Eur J Biochem*. 1999 May;262(1):12-8. doi: 10.1046/j.1432-1327.1999.00339.x. PMID: 10231358.
4. Mandelkow E, Mandelkow EM. Kinesin motors and disease. *Trends Cell Biol*. 2002 Dec;12(12):585-91. doi: 10.1016/s0962-8924(02)02400-5. PMID: 12495847.
5. Goodson HV, Kang SJ, Endow SA. Molecular phylogeny of the kinesin family of microtubule motor proteins. *J Cell Sci*. 1994 Jul;107 ( Pt 7):1875-84. doi: 10.1242/jcs.107.7.1875. PMID: 7983154.
6. Walczak CE, Mitchison TJ. Kinesin-related proteins at mitotic spindle poles: function and regulation. *Cell*. 1996 Jun 28;85(7):943-6. doi: 10.1016/s0092-8674(00)81295-7. PMID: 8674121.
7. Lawrence CJ, Dawe RK, Christie KR, Cleveland DW, Dawson SC, Endow SA, et al. A standardized kinesin nomenclature. *J Cell Biol*. 2004 Oct 11;167(1):19-22. doi: 10.1083/jcb.200408113. PMID: 15479732; PMCID: PMC2041940.
8. Blangy A, Arnaud L, Nigg EA. Phosphorylation by p34cdc2 protein kinase regulates binding of the kinesin-related motor HsEg5 to the dynactin subunit p150. *J Biol Chem*. 1997 Aug 1;272(31):19418-24. doi: 10.1074/jbc.272.31.19418. PMID: 9235942.
9. DeBonis S, Simorre JP, Crevel I, Lebeau L, Skoufias DA, Blangy A, et al. Interaction of the mitotic inhibitor monastrol with human kinesin Eg5. *Biochemistry*. 2003 Jan 21;42(2):338-49. doi: 10.1021/bi026716j. PMID: 12525161.
10. Blangy A, Lane HA, d'Hérin P, Harper M, Kress M, Nigg EA. Phosphorylation by p34cdc2 regulates spindle association of human Eg5, a kinesin-related motor essential for bipolar spindle formation in vivo. *Cell*. 1995 Dec 29;83(7):1159-69. doi: 10.1016/0092-8674(95)90142-6. PMID: 8548803.
11. Inoué S, Salmon ED. Force generation by microtubule assembly/disassembly in mitosis and related movements. *Mol Biol Cell*. 1995 Dec;6(12):1619-40. doi: 10.1091/mbc.6.12.1619. PMID: 8590794; PMCID: PMC301321.
12. Compton DA. Spindle assembly in animal cells. *Annu Rev Biochem*. 2000;69:95-114. doi: 10.1146/annurev.biochem.69.1.95. PMID: 10966454.
13. Ferhat L, Cook C, Chauviere M, Harper M, Kress M, Lyons GE, et al. Expression of the mitotic motor protein Eg5 in postmitotic neurons: implications for neuronal development. *J Neurosci*. 1998 Oct 1;18(19):7822-35. doi: 10.1523/JNEUROSCI.18-19-07822.1998. PMID: 9742151; PMCID: PMC6793023.
14. Hegde P, Cogswell J, Carrick K, Jackson J, Wood K, Eng W, et al., editors. Differential gene expression analysis of kinesin spindle protein in human solid tumors. *Proc Am Soc Clin Oncol*; 2003.
15. Carter BZ, Mak DH, Shi Y, Schober WD, Wang RY, Konopleva M, et al. Regulation and targeting of Eg5, a mitotic motor protein in blast crisis CML: overcoming imatinib resistance. *Cell Cycle*. 2006 Oct;5(19):2223-9. doi: 10.4161/cc.5.19.3255. Epub 2006 Oct 1. PMID: 16969080.
16. Hansen GM, Justice MJ. Activation of Hex and mEg5 by retroviral insertion may contribute to mouse B-cell leukemia. *Oncogene*. 1999 Nov 11;18(47):6531-9. doi: 10.1038/sj.onc.1203023. PMID: 10597256.
17. Ding S, Xing N, Lu J, Zhang H, Nishizawa K, Liu S, et al. Overexpression of Eg5 predicts unfavorable prognosis in non-muscle in-

- vasive bladder urothelial carcinoma. *Int J Urol.* 2011 Jun;18(6):432-8. doi: 10.1111/j.1442-2042.2011.02751.x. Epub 2011 Mar 30. PMID: 21449971.
18. Liu M, Wang X, Yang Y, Li D, Ren H, Zhu Q, Chen Q, Han S, Hao J, Zhou J. Ectopic expression of the microtubule-dependent motor protein Eg5 promotes pancreatic tumorigenesis. *J Pathol.* 2010 Jun;221(2):221-8. doi: 10.1002/path.2706. PMID: 20455257.
19. Castillo A, Morse HC 3rd, Godfrey VL, Naeem R, Justice MJ. Overexpression of Eg5 causes genomic instability and tumor formation in mice. *Cancer Res.* 2007 Nov 1;67(21):10138-47. doi: 10.1158/0008-5472.CAN-07-0326. PMID: 17974955.
20. Masuda A, Maeno K, Nakagawa T, Saito H, Takahashi T. Association between mitotic spindle checkpoint impairment and susceptibility to the induction of apoptosis by anti-microtubule agents in human lung cancers. *Am J Pathol.* 2003 Sep;163(3):1109-16. doi: 10.1016/S0002-9440(10)63470-0. PMID: 12937152; PMCID: PMC1868274.
21. Sarli V, Giannis A. Inhibitors of mitotic kinesins: next-generation antimetabolites. *ChemMedChem.* 2006 Mar;1(3):293-8. doi: 10.1002/cmdc.200500045. PMID: 16892362.
22. Orr GA, Verdier-Pinard P, McDaid H, Horwitz SB. Mechanisms of Taxol resistance related to microtubules. *Oncogene.* 2003 Oct 20;22(47):7280-95. doi: 10.1038/sj.onc.1206934. PMID: 14576838; PMCID: PMC4039039.
23. Joshi HC. Microtubule dynamics in living cells. *Curr Opin Cell Biol.* 1998 Feb;10(1):35-44. doi: 10.1016/s0955-0674(98)80084-7. PMID: 9484593.
24. Lane J, Allan V. Microtubule-based membrane movement. *Biochim Biophys Acta.* 1998 Jun 29;1376(1):27-55. doi: 10.1016/s0304-4157(97)00010-5. PMID: 9666066.
25. Desai A, Mitchison TJ. Microtubule polymerization dynamics. *Annu Rev Cell Dev Biol.* 1997;13:83-117. doi: 10.1146/annurev.cell.bio.13.1.83. PMID: 9442869.
26. Sakowicz R, Finer JT, Beraud C, Crompton A, Lewis E, Fritsch A, Lee Y, Mak J, Moody R, Turincio R, Chabala JC, Gonzales P, Roth S, Weitman S, Wood KW. Antitumor activity of a kinesin inhibitor. *Cancer Res.* 2004 May 1;64(9):3276-80. doi: 10.1158/0008-5472.can-03-3839. PMID: 15126370.
27. Jackson JR, Patrick DR, Dar MM, Huang PS. Targeted anti-mitotic therapies: can we improve on tubulin agents? *Nat Rev Cancer.* 2007 Feb;7(2):107-17. doi: 10.1038/nrc2049. PMID: 17251917.
28. Szakács G, Paterson JK, Ludwig JA, Booth-Genthe C, Gottesman MM. Targeting multidrug resistance in cancer. *Nat Rev Drug Discov.* 2006 Mar;5(3):219-34. doi: 10.1038/nrd1984. PMID: 16518375.
29. Yan Y, Sardana V, Xu B, Homnick C, Halczenko W, Buser CA, Schaber M, Hartman GD, Huber HE, Kuo LC. Inhibition of a mitotic motor protein: where, how, and conformational consequences. *J Mol Biol.* 2004 Jan 9;335(2):547-54. doi: 10.1016/j.jmb.2003.10.074. PMID: 14672662.
30. Rickert KW, Schaber M, Torrent M, Neilson LA, Tasber ES, Garbaccio R, et al. Discovery and biochemical characterization of selective ATP competitive inhibitors of the human mitotic kinesin KSP. *Arch Biochem Biophys.* 2008;469(2):220-31.
31. Sakowicz R, Berdelis MS, Ray K, Blackburn CL, Hopmann C, Faulkner DJ, et al. A marine natural product inhibitor of kinesin motors. *Science.* 1998 Apr 10;280(5361):292-5. doi: 10.1126/science.280.5361.292. PMID: 9535660.
32. Sarli V, Giannis A. Targeting the kinesin spindle protein: basic principles and clinical implications. *Clin Cancer Res.* 2008 Dec 1;14(23):7583-7. doi: 10.1158/1078-0432.CCR-08-0120. PMID: 19047082.
33. Jiang C, You Q. Kinesin spindle protein inhibitors in cancer: a patent review (2008 - present). *Expert Opin Ther Pat.* 2013 Dec;23(12):1547-60. doi: 10.1517/13543776.2013.833606. Epub 2013 Aug 26. PMID: 23978071.
34. Matsuno K, Sawada J-i, Asai A. Therapeutic potential of mitotic kinesin inhibitors in cancer. *Expert Opin Ther Pat.* 2008;18(3):253-74.
35. Zhang Y, Xu W. Progress on kinesin spindle protein inhibitors as anti-cancer agents. *Anti-cancer Agents Med Chem.* 2008 Aug;8(6):698-704. PMID: 18690830.
36. Knight SD, Parrish CA. Recent progress in the identification and clinical evaluation of inhibitors of the mitotic kinesin KSP.

*Curr Top Med Chem.* 2008;8(10):888-904. doi: 10.2174/156802608784911626. PMID: 18673173.

37. Huszar D, Theoclitou ME, Skolnik J, Herbst R. Kinesin motor proteins as targets for cancer therapy. *Cancer Metastasis Rev.* 2009 Jun;28(1-2):197-208. doi: 10.1007/s10555-009-9185-8. PMID: 19156502.

38. Mayer TU, Kapoor TM, Haggarty SJ, King RW, Schreiber SL, Mitchison TJ. Small molecule inhibitor of mitotic spindle bipolarity identified in a phenotype-based screen. *Science.* 1999 Oct 29;286(5441):971-4. doi: 10.1126/science.286.5441.971. PMID: 10542155..

39. Nair V. *Multicomponent Reactions.* Edited by Jieping Zhu and Hugues Bienyamé. Wiley Online Library; 2005.

40. Kappe CO. A Reexamination of the Mechanism of the Biginelli Dihydropyrimidine Synthesis. Support for an N-Acyliminium Ion Intermediate(1). *J Org Chem.* 1997 Oct 17;62(21):7201-7204. doi: 10.1021/jo971010u. PMID: 11671828.

41. PETERSEN H. Syntheses of cyclic ureas by  $\alpha$ -ureidoalkylation. *Synthesis.* 1973;1973(05):243-92.

42. Riazimontazer E, Sadeghpour H, Nadri H, Sakhteman A, Tüylü Küçükkılınç T, Miri R, et al. Design, synthesis and biological activity of novel tacrine-isatin Schiff base hybrid derivatives. *Bioorg Chem.* 2019 Aug;89:103006. doi: 10.1016/j.bioorg.2019.103006. Epub 2019 May 21. PMID: 31158577.